Available online at www.jourcc.com

Journal homepage: www.JOURCC.com

Journal of Composites and Compounds

Review of bubble and magnetically driven catalytic micro/nanomotors: Fabrication and characterization

Soolmaz Mirzazadeh Khomambazari [a], *Mohammad Yusuf* [b *], *Amirhossein Esmaeilkhanian* [c *], *Raheleh Zarei* [d]

Mahsa Hojjati [e], *Fariborz Sharifianjazi* [f], *Lili Arabuli* [g]

[a] *Faculty of Sciences, Islamic Azad University Qeshm Branch, Qeshm, Iran*
[b] *Department of Petroleum Engineering, Universiti Teknologi PETRONAS, Bandar Seri Iskandar, 32610, Malaysia*
[c] *Department of Materials and Metallurgical Engineering, Amirkabir University of Technology, Tehran, Iran*
[d] *Faculty of Chemistry, Kharazmi University, Tehran, Iran*
[e] *Faculty of Chemistry, Shahrood University of Technology, Shahrood, Semnan, Iran*
[f] *School of Science and Technology, The University of Georgia, Tbilisi, Georgia*
[g] *School of Science and Technology, Department of Natural Sciences, University of Georgia, M. Kostava str. 77a, 0171 Tbilisi, Georgia*

ABSTRACT

Micro/nanomotors (MNMs) are very unique in performing tasks and performance according to their scale. These small and versatile motors are known as promising tools in various applications. The ultimate goal is the application of MNMs in various fields, which is considered an exciting technological challenge. Chemical fuel is very reliable for the movement of MNMs. Among the various movement mechanisms that exist for these engines, bubble propulsion is one of the most important, and many engines have been investigated using this propulsion mechanism. Magnetic motors are another category of motors that move by applying a magnetic driving force and their direction of movement can be adjusted by the applied magnetic field. One of the most important challenges in the field of MNMs is the use of controlled and efficient engines, which requires the manufacturing and careful design of these engines. By incorporating of two or more engines, it is possible to benefit from the advantages of each one, and at the same time, the limitations of each one are removed and the possibility of controlling the movement of the engine is provided. In this article, we review the methods of manufacturing and characterizing MNMs which consume chemical fuel and move by bubble propulsion and also have magnetic properties and can propel by applying a magnetic field. These engines can reduce the common fuel used in chemical engines by applying magnetic driving force and switching their operation in response to changing conditions. Due to continuous innovations in this field, MNMs will profoundly impact the field of Nanorobotics.

Peer review under responsibility of UGPH.

ARTICLE INFORMATION

Article history:
Received 26 June 2022
Received in revised form 11 October 2022
Accepted 26 November 2022

Keywords:
Nanomotors
Micromotors
Bubble propulsion
Magnetic propulsion

Table of contents

* *Corresponding authors: Mohammad Yusuf; E-mail: yusufshaikh.amu@gmail.com | Amirhossein Esmaeilkhanian; Email: esmaeilkhanian-a@aut.ac.ir*

https://doi.org/10.52547/jcc.4.4.6

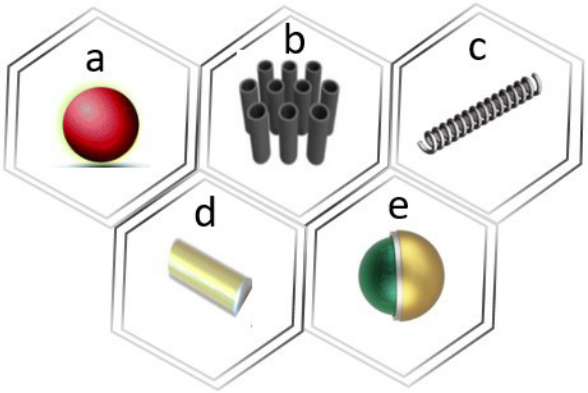

Fig. 1. Some different structures of MNMs. (a) spherical (b) tubular (c) helical (d) wire and (e) Janus.

1. Introduction

Ever since Feynman gave his speech in 1959 entitled «There's plenty of room at the bottom», a lot of research has been done on manipulation and production on very small scales. The 2016 Nobel Prize in Chemistry was awarded for the study of molecular machines, which encouraged the advancement of molecular motors. In 2002, Whitesides's [1] team created the first artificial motor on a centimeter-scale that can operate autonomously using hydrogen peroxide (H_2O_2) as fuel. This contributed significantly to the advancement of catalytic micro and nanomotors (MNMs). Later in 2004, it was announced that the size of bimetallic motors comprised of platinum and gold segments had been effectively reduced to the micrometer-level. The energy efficiency and particular surface area increase with decreasing size [2].

In the discussion of small-scale motors, in addition to the size factor, the shape and geometric structure of the engines have a significant impact on how the motors move and function. Therefore, various structures with different functions and applications were fabricated. MNMs and other subtypes of them, such as helical MNMs [3], Janus MNMs [4], nanowires [5], and microtubes [5, 6], have been successfully fabricated Fig.1 . In addition to various shapes of MNMs, propulsion and motion control of them have become increasingly the focus of research. Janus motors are based on the Janus particles, which are asymmetric structures with different physical or chemical properties. In 1991, De Gennes [7] mentioned "Janus" in his Nobel lecture with the definition of particles with two diverse hemispheres.

As mentioned, the structure of MNMs affects their motion, on the other hand, the methods of fabricating MNMs are different according to their structure, and each MNM is able to perform a specific mission according to its composition and mode of operation. The characterization and fabrication methods of MNMs still need to be greatly improved for long-term utilization. In the past years, researchers in different disciplines used two methods, top-down and bottom-up, to fabricate and develop MNMs. Fabrication techniques consist of physical vapor deposition (conventional physical vapor deposition or glancing angle deposition) [8, 9], electrochemical deposition (bipolar or template-assisted) [10], assembly [11], lithography [12], and others.

Producing MNMs with low cost and large-scale is very significant because it has an important impact on the possibility of using MNMs [13, 14].

Based on how they are created, MNMs can be divided into three categories: The MNMs may be entirely artificial, hybrid MNMs (which include natural and artificial components), or naturally occurring in organic compounds [15]. Artificial engines (self-propelled MNMs) have the capacity to transform energy from various sources into autonomous motion. These sources include ultrasonic waves [13], electric or magnetic fields [16], light [17], and chemical fuel [18].

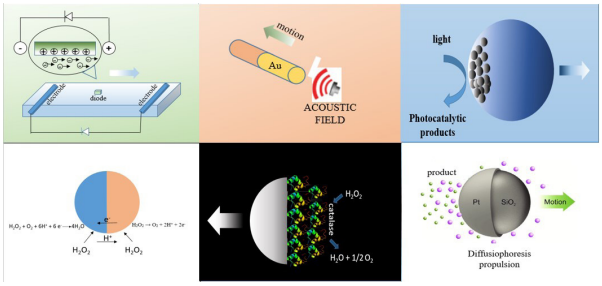

Fig. 2. Mechanisms of MNMS propulsion.

According to the various reports available in the published literature, several movement mechanisms have been proposed to describe the propulsion of MNMs [19]. The materials used in the structure of MNMs must be such that they react to the external input energy and this is a function of the desired movement mechanism. The progress of process engineering and material science in the past decades has had a significant impact on the number of contributions in the field of small-scale robotics. These impacts aim to use and combine the best materials for the propulsion of MNMs, and strategies for fabrication were considered and developed [20]. On the other hand, propulsion mechanisms have an effect on the selection of methods and routes for the fabrication of MNMs [20].

Self-electrophoresis [21], interfacial tension gradients [22], bubble propulsion [23], and diffusiophoresis [24]are among the physical and chemical mechanisms proposed to explain the propulsion behavior of MNMs. Propulsion in bubble MNMs takes place through bubbles, these bubbles are produced either through redox reactions that lead to the spontaneous production of gas or through chemical reactions that lead to the degradation of a fuel such as hydrogen peroxide or a catalysis.

Bubble propulsion is one of the most significant motion mechanisms of MNMs. Many successful cases of MNMs whose propulsion mechanism is through the bubble recoil mechanism which produced from catalytic reactions have been reported in the literature [25]. Long-term durability and precise motion control make the Bubble-propelled MNMs with favorable biocompatibility and powerful driving force suitable candidates for medical applications. Most of these MNMs simultaneously use external energy sources such as magnetic field, acoustic wave, electric field, and light to boost propulsion and control movement [25, 26].

Magnetic-propelled MNMs have drawn careful attention Due to their fuel-free actuation, remote controllability, and safety for cells and tissues, especially in the biomedical and pharmaceutical industries. Magnetic movement can be applied to nanomotors in two ways: By the transfer of magnetic torque caused by the oscillation or rotation of external magnetic fields or by applying a magnetic field gradient to induce aligned magnetophoretic motion in the same direction. This magnetic unique MNMs are favorable in the future biomedical and pharmaceutical applications because to the ease of fabrication techniques, the unrestricted choice of materials, and the successful motion control. Due to its intrinsic directionality, a magnetic field can align these particles and enable directional navigation. The most popular technique for remotely initiating and controlling the swarming activity of micro/nanoparticles with excellent biocompatibility is magnetism [27-30].

Even though the nanotechnology community is supporting this new initiative, there are still many challenges to overcome before functional MNMs are developed. Other serious challenges, such as how to control their motion and how they can be successfully driven, exist in addition to the obvious challenge of manufacturing such small devices. The degree of interest in the topic over the past 15 years has steadily gained momentum, as can be shown by the number of publications over this time period. Researchers from a variety of universities and scientific backgrounds have started tackling these challenging questions [34][31]. It is worthwhile to invest in this field of study because the mobility and

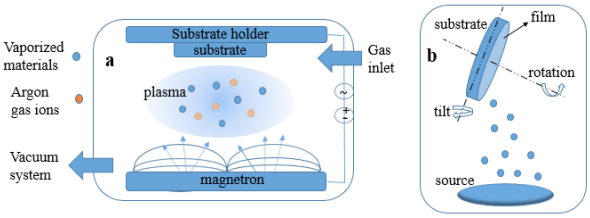

Fig. 3. (a) PVD technique and (b) GLAD technique.

control of motion of MNMs will have significant effects on future technologies [28–34].

By combining the propulsion mechanisms of bubble and magnetic, one can benefit from the advantages of both methods. In this review, we focus on various techniques/strategies for the fabrication and characterization of MNMs which drive using magnetic fields and bubble propulsion mechanisms.

2. Nano/micro motors

Any motor needs a power source to generate movement in order to function. MNMs are a category of miniaturized human-made motors that can transform chemical or external energy into mechanical motion. Most of the reported MNMs are fuel-driven. The chemical energy needed for motility in Nano-and micro-scale motors is often produced by a catalyst through the decomposition of fuel.

The catalytic decomposition of aqueous hydrogen peroxide (H_2O_2) has received considerable attention. H_2O_2 is rapidly decomposed to water and oxygen in the presence of an appropriate catalyst, often one containing platinum (Pt).

Typically, the fuel used to propel catalytic MNMs is based on H_2O_2 and N_2H_4, which are incompatible with biological systems. Several solutions, including remote-controlled motors or hybrid motors, have been proposed to address this issue. The hybrid motor was developed to combine the advantages of both motors. Fuel-free motors or remotely guided motors are efficient and simple; thus, they have been widely researched, allowing for opening up new opportunities in a variety of fields, that enable temporal, and precise spatial control. Multiple mechanisms, such as interfacial gradient propulsion, diffusiophoresis, self-electrophoresis, and bubble propulsion have been proposed to explain the autonomous mobility of fueled MNMs Fig. 2 . Magnetism, light, electricity, organism and ultrasound are the most significant external forces utilized to power MNMs [32, 33].

• Diffusiophoresis propulsion: Self-diffusiophoresis frequently refers to the propulsion of MNMs in the gradient of product concentration surrounding MNMs as a consequence of an asymmetric chemical reaction [36]. The asymmetries of catalytic MNMs play a significant role in describing motion [8]. As the collected decomposition products approach a critical threshold, which local concentration is significant and the product begins to diffuse away, the motor moves away from the catalyst. The self-diffusiophoresis propulsion could cause a particle to move at a speed of 1–10 μm/s [34]. Because of the high ionic content of biological fluids, the self-diffusiophoresis technique is not an effective choice for the fabrication of MNMs to be used in drug delivery systems [35, 36].

• Self-electrophoresis propulsion: Self-electrophoresis propulsion is typically owing to an electric gradient produced within asymmetric bimetallic conducting rods. In general, the system operates as kind of a self-contained electrochemical cell, with one metallic end functioning as the anode while the other is the cathode. It should be noticed that the highly ionic quality of biofluids might influence the self-electrophoresis mechanism, rendering them unsuitable to be utilized as drug delivery MNMs. This mechanism would include the flow of protons

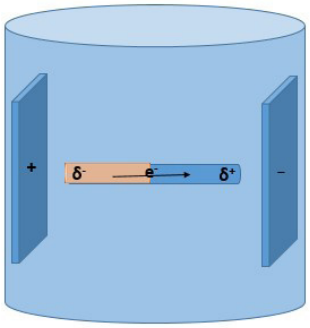

Fig. 4. Fabrication of asymmetric structure of MNMs through bipolar electrochemical deposition method.

and electrons within the particle, functioning as a galvanic cell with a short circuit. Self-electrophoresis is frequently accompanied by further plausible mechanisms [37]. The first self-electrophoresis MNMs were created by Mallouk's team [38] utilizing Ag/Pt bisegment nanorods to display directional motion behaviors toward the platinum end at a speed of approximately 10 μm/s [38].

• Ultrasound-driven motors: The application of ultrasound to drive MNMs is a relatively new development. Small-scale objects, including biological structures, may be efficiently manipulated using arbitrary wave, single beams, traveling waves, or standing waves fields. Ultrasound can be employed as an external stimulation to drive MNMs, having the advantage of non-contact. The usage of standing waves in vivo is difficult because standing waves cannot be dependably established in living organisms. Although the use of standing waves for the propulsion of MNMs is extremely advantageous, the application of standing waves in vivo is going to be difficult [39-41].

• Electrically driven motors: Electrical fields are another kind of propulsion that is garnering interest from the MNMs community. DC and AC electric fields, and also heterogeneous and homogeneous fields, can be utilized to move MNMs. Velev et al. [42] discovered that millimeter-scale semiconductor diodes can move autonomously when confronted with an external alternating electric field. The electro-osmotic flow focused all around diodes caused the diodes to move in a particular direction. Some more studies attempted to microminiaturize these diodes for additional biomedical applications using a membrane template growth method [43].

• Light-driven motors: Light can be utilized to power MNMs as an alternative source of power. In this regard, different wavelengths of light, including infrared, visible, and ultraviolet, have been employed. Furthermore, the driving mechanisms of MNMs utilizing various light sources are often distinct [37]. As light-powered MNMs, many photoactive materials, including photochromic, photothermal, and photocatalytic materials, have been utilized. Photoactive materials (In the presence of light) undergo photoisomerization, photothermal conversion, and photochemical processes to convert light energy into chemical energy or heat energy. In 2015, Guan et al. [44] utilized a simple method of dry spinning to prepare single-component TiO_2 microtubes. The motion speed of these microtubes can be adjusted easily within 0.2 s under UV irradiation. The ability to use light to drive fuel-free motors is immensely appealing, but without robust motors that can deal with the body's limited ability to absorb light across a broad spectrum, they will be limited to invasive hospital procedures [45].

• Organism-driven: Organism-driven motors are pseudo-fuel-free, and require no additional fuel for propulsion. In natural systems, certain microbes and cells, such as bacteria and sperm, may travel independently. Therefore, numerous researchers studied the feasibility of integrating them as motors into MNMs [46, 47].

MNMs with bubble propulsion mechanisms combined with a magnetic field as an external source of power source are prevalent, powerful, and extremely efficient and we will discuss them further [48].

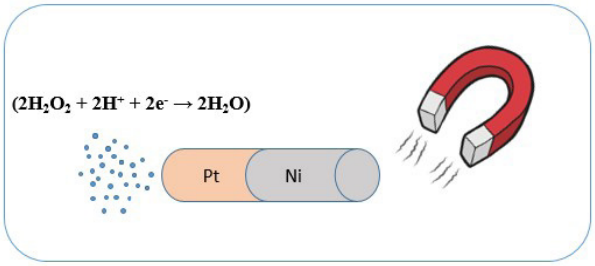

Fig. 5. magnetic and bubble propelled MNM .

3. Bubble propulsion

In the field of MNMs driving, bubble propulsion is likely the most studied mechanism. It results from the fuel decomposition spontaneously by a catalyst. The decomposition releases micron-sized gas bubbles from the MNMs surface that propels the motors away from the catalyst. Nucleation, formation of bubble, grow, and then detachment are the process at which the gaseous products would undergo. Eventually, the fluid is expelled away from the MNMs, creating the transient driving force necessary to succeed in dealing with the vicious force for self-propulsion. Continuous microbubble production and flow provide a steady driving force which is required for self-propulsion. In most of the researches, MNMs move away from the directions of bubble ejection. If well-controlled, the MNMs' motion can be aligned with the bubble ejections [49, 50].

The Bubble propulsion approach is the most commonly employed propulsion mechanism for MNMs, with applications including electrochemical analytical sensing, analytical sensing, drug delivery, the killing of pathogenic bacteria, and water purification. It has been demonstrated that bubble-propelled autonomous MNMs promote effective fluid transport and mixing, hence increasing the conventional chemical process efficiency. The microbubbles produced significantly improved localized convection and mass transport, resulting in a greater sensitivity [51-53].

Pt is a costly noble metal and the most prevalent catalytic component. Platinum decomposes hydrogen peroxide to water and oxygen.

The reduction of H_2O_2 occurs in the gold segment:

$H_2O_2 + 2H+ + 2e- \rightarrow 2H_2O$

In the platinum segment, the oxidation of the fuel O2 occurs:

$H_2O_2 \rightarrow O_2 + 2H+ + 2e-$

Other substances, such as silver and manganese oxide, are able to catalyze the decomposition of hydrogen peroxide to produce power. Alternative eco-friendly substances, including as Mg [54], Zn, Al [55], and Fe_3 react with acids and water to produce H_2 bubbles for propulsion. Some chemical agents, for instance $NaHCO_3$ (reaction with $C_4H_6O_3$), $NaBH_4$ (reaction with 4-nitrophenol pollutant), and $KMnO_4$ (reaction with H_2O_2), also generate bubbles to drive MNMs. Some precious metals, such as the iridium and gold could be utilized as engine components, and also be employed for MNMs purposes. Iridium could be utilized to catalyze the decomposition of hydrazine for bubble propelled or selfdiffusiophoresis MNMs. Palladium particles utilize as a catalyzer in order to degradation of 4-nitrophenol contaminant in a rolled-up microtubular motor and $NaBH_4$ uses as the reductant. [56-58].

By decomposing water to H_2 bubbles, the first water powered MNMs demonstrated. In the biomedical field the choice of fuel is crucial for expanding the vast uses of MNMs. Microparticles comprised of $CaCO_3$ and TXA can swim through blood by CO_2 bubble propulsion. This technique typically demands extremely cytotoxic fuels such as iodine, bromine, hydrazine, and hydrogen peroxide preventing their usage in biological applications. Recently, however, alternative fuels such as glucose or calcium carbonate ($CaCO_3$) and tranexamic acid (TXA) have been reported. [59-61].

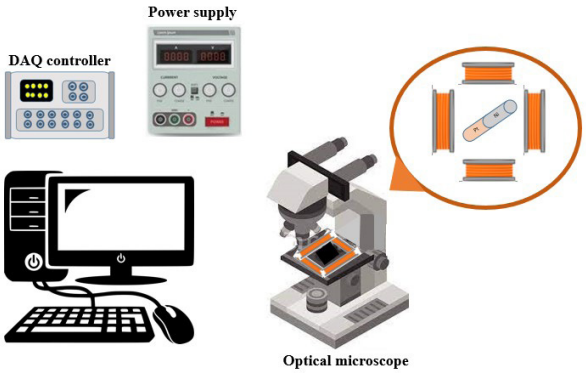

Fig. 6. schematic of the experimental workplace for actuating and visualizing magnetic MNMs.

In 2004, Sen et al. [2] utilized H_2O_2 as a fuel to drive (Pt/Au) nanorods produced using an electrochemical method, demonstrating that catalytic reactions can provide the driving forces for MNMs.

Wang et al. [62] produced the first case of Zn-based tubular micromotors driven by H_2 bubbles in acidic medium without any extra chemical fuel, which were manufactured using electro-synthesized mothered. In 2013 [63], Magnesium-based micromotors powered by the Magnesium–water reaction fabricated through ion sputtering technique. Sanchez et al. [60] created a remarkable high-performance microjet engine with bubble-driven motions exceeding 10 mm/s at physiological temperatures, their work demonstrated that bubble propulsion is a very powerful method to driving MNMs. The speed of the shell motor pushed by bubbles was significantly greater in comparison with solid and spherical motors of comparable size. The speed of MNMs depends on the ionic strength of the medium. As the salt concentration increases, the MNMs's speed reduces because a high ionic strength led to greater bubble size and fewer bubbles [41]. Surfactants play a significant role in the improved motion of bubble-propelled MNMs during the motion process by lowering interfacial free energy [64-66]. The motion behaviors of MNMs are also affected by environmental factors such as pH values, temperature, light, and other solutes.

In addition to the material biosafety, it's necessary to consider multifunctionality throughout the motors' design and construction. Self-propulsion is a very appealing method, but it has several limitations, such as a lack of directionality. Incorporating magnetic elements (such as Cobalt [67] and iron (III) oxide) into MNMs allows for accurate motion control [68, 69].

4. Magnetic MNMs

Magnetic fields are undoubtedly the most adopted form of propulsion energy for MNMs. In order to respond to the external field, magnetic materials are necessary. The majority of magnetically propelled MNMs fabricated from superparamagnetic, ferromagnetic, or ferromagnetic materials, either in form of polymer composites [70], metal, or alloys. Ni, Co, and Fe are widely used ferromagnetic materials, while Fe_2O_3 and Fe_3O_4 are regularly utilized superparamagnetic materials [71, 72].

Using electromagnetic or magnets coils, magnetic fields applied in the form of gradients, oscillation, or rotation. Utilizing gradients, which permit the application of forces to structures, is a relatively easy method of manipulating magnetic MNMs. Additionally, oscillating and rotating magnetic fields that rotate and oscillate have been utilized to propel magnetic MNMs. Considering that the magnetic materials show a magnetization axis that is mostly induced by the shape which is called shape anisotropy, rotation of the structures is possible by aligning this preferential magnetization axis synchronously. This takes place with the applied oscillating or rotating magnetic field which is created by the

Table 1.
Structure, application, manufacturing method, and salient features of recently fabricated magnetic MNMs with bubble propulsion

Materials	Fabrication Method	Structure	Fuel	Size	Application	Characterization	Important result:	Reference
Zerovalent-Iron/Pt	PVD	Janus Structure	5% H_2O_2	~1-5-μm-diameter	water purification (methylene blue)	Optical microscope (Olympus MX51) with 20× and 10× objectives and a Java-based image processing program were used to observe motion and trajectories tracking of micromotors respectively. Speed: 200 μm/s	Surfactant:TX-100 Magnetic field had influence on the motor speed	[92]
porous polystyrene sphere/NiFe/Pt	Langmuir-Blodgett/ magnetron sputtering	Janus Structure	6.3wt% H_2O_2	Size:10 μm	organics absorption and delivery (Rodamine B)	Observe motion: polarizing metallurgical microscope equipped with X10 objective and a CCD camera. magnetic field: adjustable horizontal 2D magnetic field Tracked trajectories: curved, spiral, circular. Speed: 3.3 mm/s (~320 body length). 6 successive sharp turns were achieved under magnetic control	A linear relationship between the speeds and the concentrations demonstrated.	[122]
poly(3,4-ethylene dioxythiophene)-polypyrrole/Ni/ Pt	template-directed electro-deposition	Tubular	2% H_2O_2	diameter : 5 μm	targeted hyperthermia and pollutant remediation	smooth Surface monitoring Direction and movement: light microscope equipped with a digital camera	speed reduced upon immobilization of L-asparaginase	[123]
Au/ PtCNT and Au/Pt Fe_3O_4	electrodepositing	cylindrical	15 wt % H_2O_2	diameter :220 nm	-	Average speeds :(50-60 μm/s (. Adding hydrazine:) 200 μm/s(	-	[124]
Au/Ni/Pt	layer-by-layer deposition method	concentric disk	H_2O_2	diameter :8 μm	-	The big nanoswimmer propelled forward faster than the small one at temperature < 27 °C, The small nanoswimmer moved forward faster at temperature > 27 °C.	Manipulating the propulsion path by external magnetic field	[125]
Pd/zerovalent iron/cellulose nanocrystals	Wet chemistry	cylindrical	~0.01 wt% H_2O_2	length = 825 ± 78 nm and width = 33 ± 9 nm	targeted hyperthermia and pollutant remediation	motion tracking: optical microscope equipped with CCD camera Magnetic field: small cylindrical Neodymium (NdFeB) magnets Velocity determining: Image J software H_2O_2 decomposition rate constant for Fe_2O_3<< Pd	The trajectory changed remotely with the directional change of applied field.	[126]
Pt/Ni/Au	Template-Assisted	conical tube	15% H_2O_2	50 μm diameter	Carrying magnetic cargo	the speed of the MNMs were not compromised by the cargo loading: 456μm/s (Corresponding to around three body lengths/s). movement of the magnetic guide and the pickup and transport of the large magnetic cargo facilitated by plating an intermediate layer of Ni	-	[127]
HSAMNP-PtNP MNP: Fe_3O_4 nanoparticle PtNP: platinumnanoparticle	wet templating	Microtubes	5 wt%H_2O_2 and 0.2 wt% Triton X-100,	1.20 ±0.02 μm outer diameter, ca. 23 μm Length and 124±15 nm wall thickness	capture cyanine dye and Escherichia coli	39±9 μm s^{-1} (1.7 body lengths s^{-1}) at 25 °C. Incorporation of the heavy MNP layer increased the tube weight, reduce the velocity. controlling the directional with magnetic field guidance by integrating a MNP layer in the cylinder wall	Without SDS, only one huge O_2 bubble formed, with no propulsion of the microtubes.	[128]
Fe_3O_4-Fe- zeolitic imidazolate framework-8-Pt	template-based interfacial synthesis	microrod	5 wt % H_2O_2 1 wt % SDS	diameter from 100 nm to 5 μm	Radioactive Uranium Preconcentration. Removing (96%) within 1 h	860 ± 230 μm.s^{-1} (i.e., >60 body lengths per second). magnetic response speed was related to the moving velocity of MNMs in the H_2O_2 solution	recovery under magnetic control, stable recycling ability and high selectivity	[99]

Table 1. (continued)

Materials	Fabrication Method	Structure	Fuel	Size	Application	Characterization	Important result:	Reference
poly(ε-caprolactone)-Fe_3O_4-PEG/Pt	Pickering emulsion technique	Polymeric Janus Structure nanoparticle	10 wt % H_2O_2 and 5% (w/v) NaCl 1215.78 $\mu m^2/s$	total mean size (nm): 137.2 ± 17.6	-	Indicated an erratic motion behavior. In salt-free media, NPs migrated individually, while in saline media, a collective motion occurred.	Combining magnetic- and bubble propulsion-forces influenced the motion direction of clusters.	[107]
gold-sputtered polystyrene/GO or (GDYO or BP)/ sulfhydryl group / Pt or MnO_2 NPs/Fe_2O_3 and CdSe@ ZnS	physical vapor deposition and liquid phase deposition	Janus Microparticles	5 wt % H_2O_2	~20 μm-diameter	-	the speed increases along peroxide fuel concentrations (from 5 to 10%) from 13 ± 4 to 61 ± 30 μm/s (GO), 52 ± 36 to 108 ± 35 μm/s (GDYO), and 14 ± 6 to 61 ± 29 μm/s (BP) when using Pt as catalyst. similar speeds were noted when using MnO_2 as a trigger for micromotor propulsion. After magnetic guidance the speed of Pt MNMs increase up to 75%.a lower speed increase percentage (40−50%) was noted in MnO_2MNMs in magnetic mode	In bubble-magnetic mode, clear differences can be seen among micromotors propelled by Pt or MnO_2 as a catalyst.	[108]

exerted magnetic force. By regulating the frequency of the oscillating or rotating magnetic fields, magnetic small-scale swimmers speed controlling up to a particular frequency value (step-out frequency) is possible [73].

Wu et al. [74] demonstrated that hinged structures constituted of a metallic tail connected to a magnetic head can swim along helical path by applying purely rotating magnetic fields. The structures replicate the helical klinotactic motion of particular bacteria and cells, like spermatozoa. This method is particularly promising for biomedical applications due to the diversity of ways that magnetic fields could be applied as well as their biocompatibility (low or null interaction with organic compound over a broad range of frequency values and magnetic field) [75].

Movement of NMNs through the blood [76] as well as NMNs with Janus structure in the intestine and stomach have been reported [77-80]. Another application of NMNs is their use in drug or DNA delivery. In recent studies, the functionality of NMNs inside living cells has been discussed [81, 82].

In addition to magnetic field and magnetic materials which can affect the performance of magnetic MNMs, there are some more factors affecting the motion of magnetic MNMs, for instance fluid ionic strength, viscosity, surface wettability, and geometric shape. Helical MNMs is one of the most investigated small-scale motor architectures which numerous studies have utilized rotating magnetic fields to examine its locomotion [83, 84] and Wang and colleagues [85] demonstrated a second remarkable propulsion mechanism with nanowire-based architectures like the locomotion of fish.

MNMs are made of many materials and methods to provide their needed functionality for example Magdanz et al. [86] have recently fabricated sperm-template MNMs and investigated segmented magnetization for its impact on the propulsion. The possible use of magnetic MNMs in biomedical applications is the subject of considerable research and it is needed to be more investigated [48].

5. Fabrication and characterization

5.1. Fabrication

In this section, we describe the fabrication techniques for MNMs and provide examples for each technique. Physical vapor deposition (PVD) Fig. 3.a [87] is a collection of vacuum deposition techniques in which a liquid or solid material surface is evaporated in a vacuum environment and deposited on a substrate in a thin layer. Thermal evaporation and sputtering are the most popular PVD techniques. In the PVD process, the targeted material is transferred and deposited on the surface of the substrate in a vacuum atmosphere. PVD is effective anywhere durable, pure, and extremely thin layers are required for coating [88].

Vapor deposition method results in the creation of a high pure layer and the ability to control the layer's structure, which is advantageous over alternative layering techniques for several applications. Although PVD is regarded a rather expensive technology, its use enables the fabrication of MNMs with several layers of materials with varying properties, making it one of the most common techniques for fabricating MNMs with catalytic and magnetic capabilities properties [19, 89, 90].

Fig. 3.b depicts the shape of the Glancing Angle Deposition (GLAD) [91] process, which is one of the techniques for producing thin layers. During deposition, the angle between the steam source and the substrate can be altered, enabling the formation of layers with varying thicknesses and geometries. Fe/Pt Janus Micromotors were manufactured by Chung-Seop Lee et al. [92]. As the basic particles, Fe^0 microspheres are utilized with a 50-nm-thick Pt layer coating. The Fe^0/Pt micromotors were reusable and were magnetically guided to the target pollutants using an external magnetic field. Fe^0 acted as a Fenton catalyst for the degradation of organic contaminants, while the hemispheric platinum layer catalytically degraded H_2O_2 into H_2O and O_2. PVD is a common method in order to metal decoration of MNMs, it is nonselective, expensive, and is not economically available for all metals [93].

It has been demonstrated that electrochemical deposition is a highly effective method for creating nanomaterials. Wet template synthesis employing alternative layer-by-layer assembly of proteins in a porous polycarbonate membrane is a useful technique for the development of well-designed soft protein MNMs [94]. Midway through the 1990s, Charles Martin created the membrane-template electrosynthesis technique, which has since become one of the most used electrochemical techniques for producing nanostructures. The process has proven to be incredibly effective for the fabrication of nanowires with a wide variety of chemical compositions, including semiconductor [95], polymeric [94], and metallic [96] nanowires. Initially, a thin metal coating is deposited on one side of the template to generate the electrical contact and working electrode. The membrane is subsequently assembled in an electrochemical cell. The cell has open pores facing a plating bath in order to enable wire segment deposition. The applying of a voltage to this metal film contact in the presence of an electrolyte with monomer or metal ions in order to deposition lead to the controlled growth (bottom-up) of nanowires in the template pores. Controlling the charge transferred during synthesis enables the production of nanowires with tunable lengths. Various microstructures, such as double-conical, conical, cylindrical microtubes, or as core–shell microwires, as well bilayer microtubes, have been created using the template-assisted electrochemical method. Several materials with varying predefined lengths were sequentially electrodeposited into the template pores to produce multisegment nanowires. In the membrane template-assisted electrodeposition technique, the pore wall of the template is used to shape the deposited materials, so producing the unique structure of MNMs. It is one economical method of MNMs manufacture [97, 98].

Using template-based interfacial synthesis, Yulong Ying et al. [99] synthesized a metal-organic frameworks (MOF) based micromotor. The membrane-based interfacial reaction was using to create the rod structure of zeolitic imidazolate framework-8 (ZIF-8). The stability of MOF-based motors in the presence of hydrogen peroxide and acidic environment is a significant challenge. Fe (II) doping increased the structural stability in H_2O_2 and acidic media. Using selective deposition of Pt and efficient loading of magnetic Fe_3O_4 nanoparticles, Fe-doping ZIF-8 (Fe-ZIF-8) microrods were developed to be magnetically controlled and bubble-propelled. Fe-ZIF-8 rods manufactured using a template of porous polycarbonate (PC) membrane. On top of an aqueous solution of $Zn(NO_3)_2$ or $Zn(Ac)_2$ with a predetermined concentration, polycarbonate membranes with average pore diameters of 30 nm or 100 nm were floated. After soaking the membrane for 24 hours, a 1-octanol solution of 2-MIM was carefully placed on the membrane at the interface between the two solutions. After predetermined reaction times, the membranes were removed, thoroughly washed (DI water), and dried (in air) 24 hours. Changing the experimental conditions produces distinct nanostructures of ZIF-8. At opposite ends of Fe-ZIF-8 microrods, Fe_3O_4 NPs and Pt NPs introduced using filtering and chemical techniques. Using a PC membrane with varying pore diameters, the length and diameter of the ZIF-8 rods were modified. Following the removal of the PC membrane with CH_2Cl_2 (dichloromethane), 5 μm-diameter ZIF-8 rods obtained. Before the production of ZIF-8 rods, Fe_3O_4 loaded into one side of the cylinder pores using particle filtration methods [44].

By inducing polarised deposition of conductive materials, [100] bipolar electrochemical deposition Fig. 4 can also be employed for the fabrication of MNMs. At the surface of conducting particles in solution, pH gradients are created based on the principles of bipolar electrochemistry. This enables the toposelective deposition of organic and inorganic polymer layers through a pH-activated precipitation mechanism. Due to

the process's inherent symmetry breaking, it can be employed to make Janus particles in a straightforward manner [101]. 3D laser lithography is one of the most prevalent methods for fabricating MNMs with the appropriate architecture.

Wei Zhu et al. [102] constructed functionalized artificial microfish using a quick 3D printing process (microscale continuous optical printing (μCOP)). First, Pt NPs loaded into the fish's tail for propulsion through the catalytic decomposition of hydrogen peroxide, and then Fe_3O_4 NPs loaded into the fish's head for magnetic control. The μCOP system could print three-dimensional structures in a single second with a resolution of 1 or higher, functionalized nanoparticles, biomimetic structures, and locomotive capabilities. Using in-house designed software, images of the required shape are individually loaded onto the DMD chip and projected onto photopolymerizable materials. By adjusting the cutting distances and flow rates, MNMs morphologies could be easily modified. Despite the low-cost advantage and continuous production of mass manufacturing, the output motors using this fabrication process continue to be constrained by their restricted dimension range [103].

Self-assembly, which permits the synthesis of hierarchically complex nanostructures from fundamental building blocks, is a prospective candidate strategy capable of accomplishing complex functionality at tiny scale. A directed self-assembly strategy used to synthesis magnetically steerable, autonomously moving nanomotor system. The size of nanoparticles is between five and several tens of nanometers. By coupling Fe_3O_4 NPs, Pt NPs, and Au NPs to the surface of HO- Polycaprolactone -SH Polymer single crystals (PSC) [104], a tailored polymer/nanoparticle hybrid ensemble is produced. Due to its strong catalytic activity, platinum NP is capable of propelling the entire nanomotor, which weighs approximately 100 times its own mass, at a rate of 30 μm/s. This nanomotor also enables cargo transportation and rapid remote control under a magnetic field, due to the Fe_3O_4NP ensemble on the PSC. They predicted that a diversity of end-functional polymers might be produced to construct the intelligent PSC template to which diverse nanoparticles can attach.

The majority of chemically powered catalytic nanomotors can only work in aqueous solutions with low ionic strength, because the solution conductivity decreases the axial velocity linearly. Joseph Wang et al. used a template-assisted approach that depicted a vastly simplified protocol compared to the lithographic route previously used (top-down) for fabricating rolled-up catalytic microtubes and offers a low-cost method for engineering tubular microjets comprised of various material combinations. The mechanism of oxygen-recoil propulsion of the tubular microjet motor overcame the significant ionic-strength constraint of catalytic motors with nanowire structures and enabled salt-independent motion (in one molar salt solution can propel at high speed). Placing a ferromagnetic nickel intermediate layer allowed guided motion as well as the transfer of big magnetic cargo along a preset path [103].

5.2. Characterization

This paper also discusses the prevalent characterization methods for MNMs that are utilized nowadays. The structure, size, velocity, and other relevant aspects of recently constructed magnetic MNMs with bubble propulsion are briefly summarized in Table.1, followed by a description of the characterization techniques, including monitoring, motor scale, and bubble size, etc.

Chemical propulsion lacks the level of control of magnetically powered MNMs, particularly in terms of ON/OFF motion, speed control, and directionality characteristics. The fuel-powered MNMs have been the subject of considerable effort, yet they remain unsatisfactory. Particularly for the self-electrophoresis mechanism, their movement is affected by the ion concentration of fluids and concentration of fuels. Alternatively, when the fuels exhausted, MNMs cannot undertake missions continually [105]. Fig. 5 shows a simple illustration of magnetic and bubble propelled MNM.

Although chemically propelled swimmers are beneficial for chemistry-on-the-fly applications such as water cleanup, magnetic components have been widely incorporated to provide greater controllability on the mobility features of these chemical swimmers. In addition, the disposal of MNMs into open water has a detrimental effect on the ecosystem. MNMs can be retrieved effectively by membrane separation or using an electrical external or magnetic field [106-108].

MNMs, which are composed of magnetic materials like magnetic iron oxides [109], iron, Cobalt [110], nickel [111], and their alloys [30, 112], provide magnetic control. These MNMs will orient themselves in accordance with the direction of the magnetic field and might be quickly recollected by applying an external magnetic field. Recovery of nanoparticles, like adsorbents from water, is often accomplished using membrane separation. But, membrane separation is unsuccessful for separating nanoparticles of same size. Combining photocatalysis technologies with bubble-propulsion mechanism and magnetic control will lead to highly effective environmental remediation [113].

Current work in the field of MNMs attempt to impart them with adaptable movement to increase their overall functionality in complex situations. The MNMs' structural architecture enables the incorporation of several features into a single unit for enhanced motion direction and control of their propulsion behavior with diverse energy sources to accelerate, decelerate, and reverse their navigation. According to Wang's team [48], a magnetocatalytic hybrid micromotor consists of a gold/platinum nanowire which is responsible for catalytic propulsion, with a nickel tail coupled to a silver segment which is responsible for magnetic propulsion. Using a magnetic field to counteract the impediment to the catalytic/phoretic mode's motility in salt-rich, complex environments offers tremendous promise. Thus, it can be argued that the direction of the micromotor trajectory in bubble-magnetic mode (compared to bubble-mode) allows for a more efficient distribution of the micromotor's thrusting force, resulting in faster speeds. In other words, increasing the micromotor's directionality by aligning it with a magnetic field can also contribute to a speed boost due to improved fuel interaction with active nanoparticles [114, 115].

As previously stated, MNMs have various structures, including helical, cylinders, spheres, rods, fishlike, shapeless, etc. MNMs can be examined for their size and structure using common imaging techniques such as SEM [116] and TEM [117]. AFM [118] images use to examine the surface's topography. EDS or EDX [119] analyses utilize for elemental analysis and verification of element incorporation. The capacity to control motion, alter direction, rotate, and control speed is a crucial topic and the primary advantage of employing magnetic and bubble propelled MNMs. Equipped optical utilize for motility investigation, which will be discussed further.

Besides direct motion control, magnetic fields can also be utilized to trigger hyperthermia thermophoresis and magnetoelectricity. Magnetic hyperthermia is the process of heating tumors, tissues, cells, or systems to temperatures as high as 42 °C by turning magnetic energy into heat radiation. As MNMs can be externally delivered to the infection site with the assistance of real-time image guidance (for example magnetic particle imaging scanner, clinical MRI scanner) and resulting hyperthermia treatment is localized by focusing on the tumour tissue, this function is preferred for treating cancer cells while minimizing damage to surrounding healthy tissues [120, 121]..

In another work, fluid dynamics simulations were used to evaluate the synergistic effect of bubble-propulsion in conjunction with various external stimuli (such as magnetic field and light irradiation) on the speed of micromotors. According to the findings, platinum- or manganese dioxide-based quantum dots with Fe_2O_3 NPs showed much faster bubble-light and bubble-magnetic combined motions compared

to bubble-free modes. Kaisong Yuan found that in bubble-light and bubble-magnetic modes, a built-in acceleration mechanism increases micromotor speed by up to 1.5 and 3.0 times, respectively, when a light or magnetic field is applied [108]..

The MNM produced by the group of Prodyut Dhar [126] contained Fe_2O_3/palladium NPs and cellulose nanocrystals (CNC) [129]. Based on the concept of Laplace pressure, it was anticipated that the lower diameters of bubbles created at a higher frequency by palladium NPs, on expulsion would exert a greater surface pressure on the nanomotor than the larger diameter bubbles produced by Fe_2O_3. Form the optical micrographs of Pd-FeCNC nanomotors, the development of two various sizes of bubbles by Pd and Fe_2O_3 NPs on its surface could be noticed, leading to the formation of a heterogeneous bubble gradient. Due to the disparity in bubble sizes surrounding Pd-FeCNC nanomotors, a gradient of Laplace pressure is generated across its surface, inducing a net positive thrust that results in the nanomotor's motion in a particular direction. Thus, the local pressure difference was caused by changes in the rate constant of H_2O_2 decomposition, bubble formation rate, bubble morphology, bubble growth dynamics, and bubble ejection, which resulted in a net positive driving force and nanomotor self-propulsion. The inclusion of two distinct (catalytic and magnetic) active NPs on CNC surface led in autonomous mobility of nanomotors via heterogeneous bubble propulsion mechanism, These findings were reported for the first time.

Whitesides et al. [130] introduced the first synthetic catalytic motor on a centimeter size powered by hydrogen peroxide. This research stimulated the development of MNMs by lowering the size of catalytic motors, which led to effective cargo transportation and more precise. Sen et al. [2] produced micromotors made of Pt and Au with automated motion in liquid. Wu et al. [131]created an autonomous Janus capsule motor made of partly coated dendritic Pt NPs by combining microcontact with printing template-assisted layer-by-layer self-assembly.

A typical setup platform for observing and controlling magnetically propelled MNMs includes an optical microscope, eventually connected to a high-resolution camera, a sample stage, a computer system with video capture and processing capabilities and a magnetic manipulation system. As the magnetic field source, the magnetic manipulation system comprises either electromagnets or permanent magnets. By only modifying the position and direction of a magnet, motors can be propelled through the use of a portable magnet in a straightforward manner. Although numerous researchers have documented the motion of magnetic MNMs using a single permanent magnet, operational reproducibility and precision are challenging due to the fact that magnet movement is highly dependent on the operator [132-134]. Fig. 6 shows a schematic of actuating and visualizing MNMs system.

6. Conclusion and future approach

The creation of MNMs can be aided by a deeper comprehension of their design and manufacture. In the near future, the development of robust MNMs with the capacity for precise control and orientation will enable widespread use of these vehicles. According to external or internal sources of energy, MNMs have their own unique characteristics and applications, and their limitations vary.

Magnetic MNMs tend to be particularly effective when precise movement control is required, and one of its additional benefits is the ability to separate and collect them without leaving any environmental pollutants behind. Combining these characteristics with powerful bubble propelled motors at high speeds is quite advantageous. In contrast, by combining these two categories, the limits of each thrust method can be minimized to the greatest extent possible. The problem of movement in medium with high ionic strength is one of the motion restrictions of MNMs using bubble propulsion, and the inability to control the orientation and movement of these devices restricts their uses.

The application of strong magnetic fields to boost the movement speed of magnetic MNMs is a constraint that can be overcome by combining these two propulsion mechanisms. The lower speed can also be overcome by integrating the two propulsion systems. These motors have showed significant promise for cargo applications, sensor, medicinal, and environmental. In the future, it is proposed to explore and fabricate magnetic MNMs with bubble thrust from other materials and with diverse structures and to investigate integrated motion mechanisms in order to maximize the benefits of these motors.

REFERENCES

[1] R.F. Ismagilov, A. Schwartz, N. Bowden, G.M. Whitesides, Autonomous movement and self-assembly, Angewandte Chemie International Edition 41(4) (2002) 652-654.
[2] W.F. Paxton, K.C. Kistler, C.C. Olmeda, A. Sen, S.K. St. Angelo, Y. Cao, T.E. Mallouk, P.E. Lammert, V.H. Crespi, Catalytic nanomotors: autonomous movement of striped nanorods, Journal of the American Chemical Society 126(41) (2004) 13424-13431.
[3] Y. Sun, R. Pan, Y. Chen, Y. Wang, L. Sun, N. Wang, X. Ma, G.P. Wang, Efficient Preparation of a Magnetic Helical Carbon Nanomotor for Targeted Anticancer Drug Delivery, ACS Nanoscience Au (2022).
[4] W. Liu, W. Wang, X. Dong, Y. Sun, Near-infrared light-powered janus nanomotor significantly facilitates inhibition of amyloid-β fibrillogenesis, ACS applied materials & interfaces 12(11) (2020) 12618-12628.
[5] G.Y. Karaca, F. Kuralay, E. Uygun, K. Ozaltin, S.E. Demirbuken, B. Garipcan, L. Oksuz, A.U. Oksuz, Gold–nickel nanowires as nanomotors for cancer marker biodetection and chemotherapeutic drug delivery, ACS Applied Nano Materials 4(4) (2021) 3377-3388.
[6] K. Cai, S. Sun, J. Shi, Q.-H. Qin, Carbon-nanotube Nanomotor Driven by Graphene Origami, Physical Review Applied 15(5) (2021) 054017.
[7] P.G. de Gennes, Weiche Materie.(Nobel-Vortrag), Angewandte Chemie 104(7) (1992) 856-859.
[8] Y. Deng, W. Chen, B. Li, C. Wang, T. Kuang, Y. Li, Physical vapor deposition technology for coated cutting tools: A review, Ceramics International 46(11) (2020) 18373-18390.
[9] A. Nath, B.K. Mahajan, L.R. Singh, S. Vishwas, R.K. Nanda, M.B. Sarkar, Enhancing detectivity of indium-oxide-based photodetectors via vertical nanostructuring through glancing angle deposition, Journal of Electronic Materials 50(6) (2021) 3722-3730.
[10] R. Lin, W. Yu, X. Chen, H. Gao, Self-Propelled Micro/Nanomotors for Tumor Targeting Delivery and Therapy, Advanced Healthcare Materials 10(1) (2021) 2001212.
[11] Wang, Z., et al., Fluidity-Guided Assembly of Au@ Pt on Liposomes as a Catalase-Powered Nanomotor for Effective Cell Uptake in Cancer Cells and Plant Leaves. ACS nano, 2022. 16(6): p. 9019-9030.
[12] S.T. Howell, A. Grushina, F. Holzner, J. Brugger, Thermal scanning probe lithography—A review, Microsystems & nanoengineering 6(1) (2020) 1-24.
[13] L. Hu, N. Wang, K. Tao, Catalytic Micro/Nanomotors: Propulsion Mechanisms, Fabrication, Control, and Applications, Smart nanosystems for biomedicine, optoelectronics and catalysis, IntechOpen2020.
[14] J. Sun, H. Tan, S. Lan, F. Peng, Y. Tu, Progress on the fabrication strategies of self-propelled micro/nanomotors, JCIS Open 2 (2021) 100011.
[15] Y. Hu, Z. Li, Y. Sun, Ultrasmall enzyme/light-powered nanomotor facilitates cholesterol detection, Journal of Colloid and Interface Science 621 (2022) 341-351.
[16] Z. Liu, T. Xu, M. Wang, C. Mao, B. Chi, Magnetic mesoporous silica/ε-polylysine nanomotor-based removers of blood Pb^{2+}, Journal of Materials Chemistry B 8(48) (2020) 11055-11062.
[17] F. Ji, B. Wang, L. Zhang, Light-triggered catalytic performance enhancement using magnetic nanomotor ensembles, Research 2020 (2020).
[18] T. Kwon, N. Kumari, A. Kumar, J. Lim, C.Y. Son, I.S. Lee, Au/Pt-egg-in-Nest nanomotor for glucose-powered catalytic motion and enhanced molecular transport to living cells, Angewandte Chemie International Edition 60(32) (2021) 17579-17586.
[19] J. Gibbs, Y. Zhao, Catalytic nanomotors: fabrication, mechanism, and applications, Frontiers of Materials Science 5(1) (2011) 25-39.
[20] S. Pané, P. Wendel-Garcia, Y. Belce, X.-Z. Chen, J. Puigmartí-Luis, Powering and Fabrication of Small-Scale Robotics Systems, Current Robotics Reports (2021) 1-14.

[21] L. Cai, D. Xu, H. Chen, L. Wang, Y. Zhao, Designing bioactive micro-/nano-motors for engineered regeneration, Engineered Regeneration 2 (2021) 109-115.
[22] A.D. Fusi, Y. Li, A. Llopis-Lorente, T. Patiño, J.C. van Hest, L. Abdelmohsen, Achieving Control in Micro-/Nanomotor Mobility, Angewandte Chemie (2022).
[23] T. Wang, M. Zheng, L. Wang, L. Ji, S. Wang, Crucial role of an aerophobic substrate in bubble-propelled nanomotor aggregation, Nanotechnology 31(35) (2020) 355504.
[24] Y. Xing, M. Zhou, T. Xu, S. Tang, Y. Fu, X. Du, L. Su, Y. Wen, X. Zhang, T. Ma, Core@ Satellite Janus Nanomotors with pH-Responsive Multi-phoretic Propulsion, Angewandte Chemie International Edition 59(34) (2020) 14368-14372.
[25] Y. Zhou, L. Dai, N. Jiao, Review of Bubble Applications in Microrobotics: Propulsion, Manipulation, and Assembly, Micromachines 13(7) (2022) 1068.
[26] V. Pal Singh Sidhu, R. Borges, M. Yusuf, S. Mahmoudi, S. Fallah Ghorbani, M. Hosseinikia, P. Salahshour, F. Sadeghi, M. Arefian, A comprehensive review of bioactive glass: synthesis, ion substitution, application, challenges, and future perspectives, Journal of Composites and Compounds 3(9) (2021) 247-261.
[27] P. Zhang, G. Wu, C. Zhao, L. Zhou, X. Wang, S. Wei, Magnetic stomatocyte-like nanomotor as photosensitizer carrier for photodynamic therapy based cancer treatment, Colloids and Surfaces B: Biointerfaces 194 (2020) 111204.
[28] Y. Shen, W. Zhang, G. Li, P. Ning, Z. Li, H. Chen, X. Wei, X. Pan, Y. Qin, B. He, Adaptive control of nanomotor swarms for magnetic-field-programmed cancer cell destruction, ACS nano 15(12) (2021) 20020-20031.
[29] M.K. Manshadi, M. Saadat, M. Mohammadi, M. Shamsi, M. Dejam, R. Kamali, A. Sanati-Nezhad, Delivery of magnetic micro/nanoparticles and magnetic-based drug/cargo into arterial flow for targeted therapy, Drug delivery 25(1) (2018) 1963-1973.
[30] A.R. Rouhani, A.H. Esmaeil-Khanian, F. Davar, S. Hasani, The effect of agarose content on the morphology, phase evolution, and magnetic properties of CoFe2O4 nanoparticles prepared by sol-gel autocombustion method, International Journal of Applied Ceramic Technology 15(3) (2018) 758-765.
[31] J. Wang, K.M. Manesh, Motion control at the nanoscale, Small 6(3) (2010) 338-345.
[32] A. Mallick, A. Laskar, R. Adhikari, S. Roy, Redox reaction triggered nanomotors based on soft-oxometalates with high and sustained motility, Frontiers in chemistry 6 (2018) 152.
[33] M. Safdar, S.U. Khan, J. Jänis, Progress toward catalytic micro-and nanomotors for biomedical and environmental applications, Advanced Materials 30(24) (2018) 1703660.
[34] H. Ye, Y. Wang, D. Xu, X. Liu, S. Liu, X. Ma, Design and fabrication of micro/nano-motors for environmental and sensing applications, Applied Materials Today 23 (2021) 101007.
[35] Y. Xing, X. Du, T. Xu, X. Zhang, Janus dendritic silica/carbon@ Pt nanomotors with multiengines for H2O2, near-infrared light and lipase powered propulsion, Soft Matter 16(41) (2020) 9553-9558.
[36] Z. Kheradmand, M. Rabiei, A. Noori Tahneh, E. Shirali, M. Abedi, B. Dashtipour, E. Barati, Targeted drug delivery by bone cements, Journal of Composites and Compounds 4(10) (2022) 59-73.
[37] Y. Wang, R.M. Hernandez, D.J. Bartlett, J.M. Bingham, T.R. Kline, A. Sen, T.E. Mallouk, Bipolar electrochemical mechanism for the propulsion of catalytic nanomotors in hydrogen peroxide solutions, Langmuir 22(25) (2006) 10451-10456.
[38] W.F. Paxton, P.T. Baker, T.R. Kline, Y. Wang, T.E. Mallouk, A. Sen, Catalytically induced electrokinetics for motors and micropumps, Journal of the American Chemical Society 128(46) (2006) 14881-14888.
[39] M. Leal-Estrada, M. Valdez-Garduño, F. Soto, V. Garcia-Gradilla, Engineering ultrasound fields to power medical micro/nanorobots, Current Robotics Reports 2(1) (2021) 21-32.
[40] L. Meng, F. Cai, F. Li, W. Zhou, L. Niu, H. Zheng, Acoustic tweezers, Journal of Physics D: Applied Physics 52(27) (2019) 273001.
[41] D. Ahmed, T. Baasch, B. Jang, S. Pane, J. Dual, B.J. Nelson, Artificial swimmers propelled by acoustically activated flagella, Nano letters 16(8) (2016) 4968-4974.
[42] S.T. Chang, V.N. Paunov, D.N. Petsev, O.D. Velev, Remotely powered self-propelling particles and micropumps based on miniature diodes, Nature materials 6(3) (2007) 235-240.
[43] L. Liu, J. Gao, D.A. Wilson, Y. Tu, F. Peng, Fuel-Free Micro-/Nanomotors as Intelligent Therapeutic Agents, Chemistry–An Asian Journal 14(14) (2019) 2325-2335.
[44] F. Mou, Y. Li, C. Chen, W. Li, Y. Yin, H. Ma, J. Guan, Single-Component TiO2 Tubular Microengines with Motion Controlled by Light-Induced Bubbles, Small 11(21) (2015) 2564-2570.
[45] L.K. Abdelmohsen, F. Peng, Y. Tu, D.A. Wilson, Micro-and nano-motors for biomedical applications, Journal of Materials Chemistry B 2(17) (2014) 2395-2408.
[46] V. Magdanz, S. Sanchez, O.G. Schmidt, Development of a sperm-flagella driven micro-bio-robot, Advanced materials 25(45) (2013) 6581-6588.
[47] R. Blakemore, Magnetotactic bacteria, Science 190(4212) (1975) 377-379.
[48] W. Gao, K.M. Manesh, J. Hua, S. Sattayasamitsathit, J. Wang, Hybrid nanomotor: A catalytically/magnetically powered adaptive nanowire swimmer, Small 7(14) (2011) 2047-2051.
[49] M. Zeng, D. Huang, P. Wang, D. King, B. Peng, J. Luo, Q. Lei, L. Zhang, L. Wang, A. Shinde, Autonomous catalytic nanomotors based on 2D magnetic nanoplates, ACS Applied Nano Materials 2(3) (2019) 1267-1273.
[50] S. Sánchez, L. Soler, J. Katuri, Chemically powered micro-and nanomotors, Angewandte Chemie International Edition 54(5) (2015) 1414-1444.
[51] W. Gao, X. Feng, A. Pei, Y. Gu, J. Li, J. Wang, Seawater-driven magnesium based Janus micromotors for environmental remediation, Nanoscale 5(11) (2013) 4696-4700.
[52] J.A. Delezuk, D.E. Ramírez-Herrera, B.E.-F. de Ávila, J. Wang, Chitosan-based water-propelled micromotors with strong antibacterial activity, Nanoscale 9(6) (2017) 2195-2200.
[53] T. Xu, F. Soto, W. Gao, R. Dong, V. Garcia-Gradilla, E. Magaña, X. Zhang, J. Wang, Reversible swarming and separation of self-propelled chemically powered nanomotors under acoustic fields, Journal of the American Chemical Society 137(6) (2015) 2163-2166.
[54] F. Niazvand, A. Cheshmi, M. Zand, R. NasrAzadani, B. Kumari, A. Raza, S. Nasibi, An overview of the development of composites containing Mg and Zn for drug delivery, Journal of Composites and Compounds 2(5) (2020) 193-204.
[55] A. Abuchenari, F. Sharifianjazi, A. Pakseresht, M. Pudineh, A. Esmaeilkhanian, Effect of aluminum on microstructural and magnetic properties of nanostructured (Fe85Ni15)97Al3 alloy produced via mechanical alloying, Advanced Powder Technology 32(2) (2021) 337-345.
[56] W. Gao, A. Pei, J. Wang, Water-driven micromotors, ACS nano 6(9) (2012) 8432-8438.
[57] S.K. Srivastava, M. Guix, O.G. Schmidt, Wastewater mediated activation of micromotors for efficient water cleaning, Nano letters 16(1) (2016) 817-821.
[58] W. Gao, A. Pei, R. Dong, J. Wang, Catalytic iridium-based Janus micromotors powered by ultralow levels of chemical fuels, Journal of the American Chemical Society 136(6) (2014) 2276-2279.
[59] J.R. Baylis, J.H. Yeon, M.H. Thomson, A. Kazerooni, X. Wang, A.E. St. John, E.B. Lim, D. Chien, A. Lee, J.Q. Zhang, Self-propelled particles that transport cargo through flowing blood and halt hemorrhage, Science advances 1(9) (2015) e1500379.
[60] X. Ma, A. Jannasch, U.-R. Albrecht, K. Hahn, A. Miguel-López, E. Schaffer, S. Sánchez, Enzyme-powered hollow mesoporous Janus nanomotors, Nano letters 15(10) (2015) 7043-7050.
[61] R. Nasr Azadani, M. Sabbagh, H. Salehi, A. Cheshmi, A. Raza, B. Kumari, G. Erabi, Sol-gel: Uncomplicated, routine and affordable synthesis procedure for utilization of composites in drug delivery: Review, Journal of Composites and Compounds 3(6) (2021) 57-70.
[62] W. Gao, A. Uygun, J. Wang, Hydrogen-bubble-propelled zinc-based microrockets in strongly acidic media, Journal of the American Chemical Society 134(2) (2012) 897-900.
[63] F. Mou, C. Chen, H. Ma, Y. Yin, Q. Wu, J. Guan, Self-propelled micromotors driven by the magnesium–water reaction and their hemolytic properties, Angewandte Chemie International Edition 52(28) (2013) 7208-7212.
[64] H. Wang, X. Gu, C. Wang, Self-propelling hydrogel/emulsion-hydrogel soft motors for water purification, ACS Applied Materials & Interfaces 8(14) (2016) 9413-9422.
[65] J. Simmchen, Movement at the nanoscale: Catalytically and light driven micromotors, Universitat Autònoma de Barcelona2015.
[66] F. Mazur, Bio-inspired Liposome-based Platforms for Biomedical Applications, UNSW Sydney, 2021.
[67] M. Radmansouri, E. Bahmani, E. Sarikhani, K. Rahmani, F. Sharifianjazi, M. Irani, Doxorubicin hydrochloride - Loaded electrospun chitosan/cobalt ferrite/titanium oxide nanofibers for hyperthermic tumor cell treatment and controlled drug release, International Journal of Biological Macromolecules 116 (2018) 378-384.
[68] D. Vilela, M.M. Stanton, J. Parmar, S. Sánchez, Microbots decorated with silver nanoparticles kill bacteria in aqueous media, ACS applied materials & interfaces 9(27) (2017) 22093-22100.
[69] P. Abasian, M. Radmansouri, M. Habibi Jouybari, M.V. Ghasemi, A. Mohammadi, M. Irani, F.S. Jazi, Incorporation of magnetic NaX zeolite/DOX into the PLA/chitosan nanofibers for sustained release of doxorubicin against carcinoma cells death in vitro, International Journal of Biological Macromolecules 121 (2019)

398-406.
[70] F. Niazvand, P.R. Wagh, E. Khazraei, M. Borzouyan Dastjerdi, C. Patil, I.A. Najar, Application of carbon allotropes composites for targeted cancer therapy drugs: A review, Journal of Composites and Compounds 3(7) (2021) 140-151.
[71] K.E. Peyer, L. Zhang, B.J. Nelson, Bio-inspired magnetic swimming microrobots for biomedical applications, Nanoscale 5(4) (2013) 1259-1272.
[72] K.E. Peyer, S. Tottori, F. Qiu, L. Zhang, B.J. Nelson, Magnetic helical micromachines, Chemistry–A European Journal 19(1) (2013) 28-38.
[73] B. Jang, A. Hong, C. Alcantara, G. Chatzipirpiridis, X. Marti, E. Pellicer, J. Sort, Y. Harduf, Y. Or, B.J. Nelson, Programmable locomotion mechanisms of nanowires with semihard magnetic properties near a surface boundary, ACS applied materials & interfaces 11(3) (2018) 3214-3223.
[74] J. Wu, B. Jang, Y. Harduf, Z. Chapnik, Ö.B. Avci, X. Chen, J. Puigmartí-Luis, O. Ergeneman, B.J. Nelson, Y. Or, Helical Klinotactic Locomotion of Two-Link Nanoswimmers with Dual-Function Drug-Loaded Soft Polysaccharide Hinges, Advanced Science 8(8) (2021) 2004458.
[75] F. Sharifianjazi, M. Irani, A. Esmaeilkhanian, L. Bazli, M.S. Asl, H.W. Jang, S.Y. Kim, S. Ramakrishna, M. Shokouhimehr, R.S. Varma, Polymer incorporated magnetic nanoparticles: Applications for magnetoresponsive targeted drug delivery, Materials Science and Engineering: B 272 (2021) 115358.
[76] P.L. Venugopalan, R. Sai, Y. Chandorkar, B. Basu, S. Shivashankar, A. Ghosh, Conformal cytocompatible ferrite coatings facilitate the realization of a nanovoyager in human blood, Nano letters 14(4) (2014) 1968-1975.
[77] W. Gao, R. Dong, S. Thamphiwatana, J. Li, W. Gao, L. Zhang, J. Wang, Artificial micromotors in the mouse's stomach: A step toward in vivo use of synthetic motors, ACS nano 9(1) (2015) 117-123.
[78] B.E.-F. de Ávila, P. Angsantikul, J. Li, M. Angel Lopez-Ramirez, D.E. Ramírez-Herrera, S. Thamphiwatana, C. Chen, J. Delezuk, R. Samakapiruk, V. Ramez, Micromotor-enabled active drug delivery for in vivo treatment of stomach infection, Nature communications 8(1) (2017) 1-9.
[79] X. Wei, M. Beltrán-Gastélum, E. Karshalev, B. Esteban-Fernández de Ávila, J. Zhou, D. Ran, P. Angsantikul, R.H. Fang, J. Wang, L. Zhang, Biomimetic micromotor enables active delivery of antigens for oral vaccination, Nano letters 19(3) (2019) 1914-1921.
[80] L. Kong, N.F. Rosli, H.L. Chia, J. Guan, M. Pumera, Self-propelled autonomous Mg/Pt Janus micromotor interaction with human cells, Bulletin of the Chemical Society of Japan 92(10) (2019) 1754-1758.
[81] M. Pal, N. Somalwar, A. Singh, R. Bhat, S.M. Eswarappa, D.K. Saini, A. Ghosh, Maneuverability of magnetic nanomotors inside living cells, Advanced Materials 30(22) (2018) 1800429.
[82] M. Pal, D. Dasgupta, N. Somalwar, V. Reshma, M. Tiwari, D. Teja, S.M. Narayana, A. Katke, R. Jayshree, R. Bhat, Helical nanobots as mechanical probes of intra-and extracellular environments, Journal of Physics: Condensed Matter 32(22) (2020) 224001.
[83] X.-Z. Chen, M. Hoop, F. Mushtaq, E. Siringil, C. Hu, B.J. Nelson, S. Pané, Recent developments in magnetically driven micro-and nanorobots, Applied Materials Today 9 (2017) 37-48.
[84] S. Tottori, L. Zhang, F. Qiu, K.K. Krawczyk, A. Franco-Obregón, B.J. Nelson, Magnetic helical micromachines: fabrication, controlled swimming, and cargo transport, Advanced materials 24(6) (2012) 811-816.
[85] J. Li, S. Sattayasamitsathit, R. Dong, W. Gao, R. Tam, X. Feng, S. Ai, J. Wang, Template electrosynthesis of tailored-made helical nanoswimmers, Nanoscale 6(16) (2014) 9415-9420.
[86] V. Magdanz, J. Vivaldi, S. Mohanty, A. Klingner, M. Vendittelli, J. Simmchen, S. Misra, I.S. Khalil, Impact of Segmented Magnetization on the Flagellar Propulsion of Sperm-Templated Microrobots, Advanced science 8(8) (2021) 2004037.
[87] J.E. Mahan, Physical vapor deposition of thin films, 2000.
[88] J. Singh, D.E. Wolfe, Review Nano and macro-structured component fabrication by electron beam-physical vapor deposition (EB-PVD), Journal of materials Science 40(1) (2005) 1-26.
[89] H. Duan, L. Heng, X. Ou, H. Zhang, H. Guo, L. Fan, L. Hu, K. Jiang, Magnesium-coated hydroxyapatite/titania cement as a potential nanomotor-based coating on orthopedic implant, Materials Letters 316 (2022) 132042.
[90] S. Khoee, S. Moayeri, M.A. Charsooghi, Self-/Magnetic-Propelled Catalytic Nanomotors Based on a Janus SPION@ PEG-Pt/PCL Hybrid Nanoarchitecture: Single-Particle versus Collective Motions, Langmuir 37(36) (2021) 10668-10682.
[91] H. Wang, M. Pumera, Fabrication of micro/nanoscale motors, Chemical reviews 115(16) (2015) 8704-8735.
[92] C.-S. Lee, J. Gong, D.-S. Oh, J.-R. Jeon, Y.-S. Chang, Zerovalent-iron/platinum Janus micromotors with spatially separated functionalities for efficient water decontamination, ACS Applied Nano Materials 1(2) (2018) 768-776.
[93] J. Gibbs, Catalytic nanomotors: fabrication by dynamic shadowing growth, propulsion mechanism, and motion characterization, University of Georgia, 2011.
[94] S. Hermanová, M. Pumera, Polymer platforms for micro-and nanomotor fabrication, Nanoscale 10(16) (2018) 7332-7342.
[95] D. Zhou, Y. Gao, H. Liu, G. Zhang, L. Li, Light-Induced Patterned Self-Assembly Behavior of Isotropic Semiconductor Nanomotors, Chemistry–An Asian Journal 14(14) (2019) 2445-2449.
[96] T.R. Kline, W.F. Paxton, T.E. Mallouk, A. Sen, Catalytic nanomotors: remote-controlled autonomous movement of striped metallic nanorods, Angewandte Chemie International Edition 44(5) (2005) 744-746.
[97] J. Wang, 9; S. Fournier-Bidoz, AC Arsenault, I. Manners and GA Ozin, Chem. Commun (2005) 441-443.
[98] J.B.H. Tok, F.Y. Chuang, M.C. Kao, K.A. Rose, S.S. Pannu, M.Y. Sha, G. Chakarova, S.G. Penn, G.M. Dougherty, Metallic striped nanowires as multiplexed immunoassay platforms for pathogen detection, Angewandte Chemie International Edition 45(41) (2006) 6900-6904.
[99] Y. Ying, A.M. Pourrahimi, Z.k. Sofer, S. Matějková, M. Pumera, Radioactive uranium preconcentration via self-propelled autonomous microrobots based on metal–organic frameworks, ACS nano 13(10) (2019) 11477-11487.
[100] F. Gholami, M. Shamsipur, A. Pashabadi, A one-pot rotational DC-bipolar approach for fabricating artistic metallic carpets, Scientific Reports 12(1) (2022) 1-8.
[101] G. Loget, J. Roche, E. Gianessi, L. Bouffier, A. Kuhn, Indirect Bipolar Electrodeposition, Journal of the American Chemical Society 134(49) (2012) 20033-20036 DOI: 10.1021/ja310400f.
[102] W. Zhu, J. Li, Y.J. Leong, I. Rozen, X. Qu, R. Dong, Z. Wu, W. Gao, P.H. Chung, J. Wang, 3D-printed artificial microfish, Advanced materials 27(30) (2015) 4411-4417.
[103] S. Liu, C. Gao, F. Peng, Micro/nanomotors in regenerative medicine, Materials Today Advances 16 (2022) 100281.
[104] Z. Amini, S.S. Rudsary, S.S. Shahraeini, B.F. Dizaji, P. Goleij, A. Bakhtiari, M. Irani, F. Sharifianjazi, Magnetic bioactive glasses/Cisplatin loaded-chitosan (CS)-grafted- poly (ε-caprolactone) nanofibers against bone cancer treatment, Carbohydrate Polymers 258 (2021) 117680.
[105] F. Mushtaq, A. Asani, M. Hoop, X.Z. Chen, D. Ahmed, B.J. Nelson, S. Pané, Highly efficient coaxial TiO2-PtPd Tubular nanomachines for photocatalytic water purification with multiple locomotion strategies, Advanced Functional Materials 26(38) (2016) 6995-7002.
[106] J. Parmar, D. Vilela, E. Pellicer, D. Esqué-de los Ojos, J. Sort, S. Sánchez, Reusable and long-lasting active microcleaners for heterogeneous water remediation, Advanced Functional Materials 26(23) (2016) 4152-4161.
[107] S. Khoee, S. Moayeri, M.A. Charsooghi, Self-/Magnetic-Propelled Catalytic Nanomotors Based on a Janus SPION@PEG-Pt/PCL Hybrid Nanoarchitecture: Single-Particle versus Collective Motions, Langmuir 37(36) (2021) 10668-10682.
[108] K. Yuan, V. de la Asuncion-Nadal, B. Jurado-Sanchez, A. Escarpa, 2D Nanomaterials wrapped janus micromotors with built-in multiengines for bubble, magnetic, and light driven propulsion, Chemistry of Materials 32(5) (2020) 1983-1992.
[109] H. Emadi, A. Hemmati, E. Behrouzi, Investigation of Fe3O4/SBA-15 magnetic nanocomposite synthesized by microwave-assisted solvothermal route as multi-therapeutic agent, Journal of Composites and Compounds 4(12) (2022) 141-144.
[110] F. Sharifianjazi, M. Moradi, N. Parvin, A. Nemati, A. Jafari Rad, N. Sheysi, A. Abouchenari, A. Mohammadi, S. Karbasi, Z. Ahmadi, A. Esmaeilkhanian, M. Irani, A. Pakseresht, S. Sahmani, M. Shahedi Asl, Magnetic CoFe2O4 nanoparticles doped with metal ions: A review, Ceramics International 46(11, Part B) (2020) 18391-18412.
[111] A. Abuchenari, M. Moradi, The Effect of Cu-substitution on the microstructure and magnetic properties of Fe-15%Ni alloy prepared by mechanical alloying, Journal of Composites and Compounds 1(1) (2019) 10-15.
[112] S. Mohammadi, Z. Mohammadi, Functionalized NiFe2O4/mesopore silica anchored to guanidine nanocomposite as a catalyst for synthesis of 4H-chromenes under ultrasonic irradiation, Journal of Composites and Compounds 3(7) (2021) 84-90.
[113] T. Maric, M.Z.M. Nasir, Y. Wang, B. Khezri, M. Pumera, Corrosion due to ageing influences the performance of tubular platinum microrobots, Nanoscale 10(3) (2018) 1322-1325.
[114] L. Ren, W. Wang, T.E. Mallouk, Two forces are better than one: combining chemical and acoustic propulsion for enhanced micromotor functionality, Accounts of chemical research 51(9) (2018) 1948-1956.
[115] C. Chen, F. Soto, E. Karshalev, J. Li, J. Wang, Hybrid nanovehicles: one machine, two engines, Advanced Functional Materials 29(2) (2019) 1806290.
[116] G. Jenkinson, Image analysis takes off, Nature 316(6023) (1985) 87-88.
[117] D. Kim, J.S. Lee, C.M. Barry, J.L. Mead, Microscopic measurement of the

degree of mixing for nanoparticles in polymer nanocomposites by TEM images, Microscopy research and technique 70(6) (2007) 539-546.
[118] L.W. Francis, P.D. Lewis, C.J. Wright, R.S. Conlan, Atomic force microscopy comes of age, Biology of the Cell 102(2) (2010) 133-143.
[119] S. Rades, V.-D. Hodoroaba, T. Salge, T. Wirth, M.P. Lobera, R.H. Labrador, K. Natte, T. Behnke, T. Gross, W.E. Unger, High-resolution imaging with SEM/T-SEM, EDX and SAM as a combined methodical approach for morphological and elemental analyses of single engineered nanoparticles, RSC advances 4(91) (2014) 49577-49587.
[120] B. Wang, K.F. Chan, J. Yu, Q. Wang, L. Yang, P.W.Y. Chiu, L. Zhang, Reconfigurable swarms of ferromagnetic colloids for enhanced local hyperthermia, Advanced Functional Materials 28(25) (2018) 1705701.
[121] Q. Wang, B. Wang, J. Yu, K. Schweizer, B.J. Nelson, L. Zhang, Reconfigurable magnetic microswarm for thrombolysis under ultrasound imaging, 2020 IEEE International Conference on Robotics and Automation (ICRA), IEEE, 2020, pp. 10285-10291.
[122] F. Wu, D. Yang, X. Huang, L. Yi, M. Liu, L. Pan, Ultrafast bubble-propelled and magnetic-field-navigated porous catalytic Janus micromotor, Journal of Nanoscience and Nanotechnology 19(7) (2019) 4154-4159.
[123] S. Evli, B. Öndeş, M. Uygun, D.A. Uygun, Asparaginase immobilized, magnetically guided, and bubble-propelled micromotors, Process Biochemistry 108 (2021) 103-109.
[124] R. Laocharoensuk, J. Burdick, J. Wang, Carbon-nanotube-induced acceleration of catalytic nanomotors, ACS nano 2(5) (2008) 1069-1075.
[125] L. Hu, J. Miao, G. Grüber, Temperature effects on disk-like gold-nickel-platinum nanoswimmer's propulsion fuelled by hydrogen peroxide, Sensors and Actuators B: Chemical 239 (2017) 586-596.
[126] P. Dhar, S. Narendren, S.S. Gaur, S. Sharma, A. Kumar, V. Katiyar, Self-propelled cellulose nanocrystal based catalytic nanomotors for targeted hyperthermia and pollutant remediation applications, International journal of biological macromolecules 158 (2020) 1020-1036.
[127] K.M. Manesh, M. Cardona, R. Yuan, M. Clark, D. Kagan, S. Balasubramanian, J. Wang, Template-assisted fabrication of salt-independent catalytic tubular microengines, ACS nano 4(4) (2010) 1799-1804.
[128] S. Kobayakawa, Y. Nakai, M. Akiyama, T. Komatsu, Self-Propelled Soft Protein Microtubes with a Pt Nanoparticle Interior Surface, Chemistry–A European Journal 23(21) (2017) 5044-5050.
[129] H. Nargesi khoramabadi, M. Arefian, M. Hojjati, I. Tajzad, A. Mokhtarzade, M. Mazhar, A. Jamavari, A review of Polyvinyl alcohol / Carboxymethyl cellulose (PVA/CMC) composites for various applications, Journal of Composites and Compounds 2(3) (2020) 69-76.
[130] Y. Ye, J. Luan, M. Wang, Y. Chen, D.A. Wilson, F. Peng, Y. Tu, Fabrication of self-propelled micro-and nanomotors based on Janus structures, Chemistry–A European Journal 25(37) (2019) 8663-8680.
[131] Y. Wu, Z. Wu, X. Lin, Q. He, J. Li, Autonomous movement of controllable assembled Janus capsule motors, ACS nano 6(12) (2012) 10910-10916.
[132] J.J. Abbott, E. Diller, A.J. Petruska, Magnetic methods in robotics, Annual Review of Control, Robotics, and Autonomous Systems 3(1) (2020) 57-90.
[133] J. Jiang, L. Yang, L. Zhang, Closed-Loop Control of a Helmholtz Coil System for Accurate Actuation of Magnetic Microrobot Swarms, IEEE Robotics and Automation Letters 6(2) (2021) 827-834.
[134] Z. Yang, L. Yang, M. Zhang, Q. Wang, S.C.H. Yu, L. Zhang, Magnetic Control of a Steerable Guidewire Under Ultrasound Guidance Using Mobile Electromagnets, IEEE Robotics and Automation Letters 6(2) (2021) 1280-1287.